ACCSCIENCE PUBLISHING

Tumor Discovery

ORIGINAL RESEARCH ARTICLE

Bioinformatics analysis of missense mutations in CXCR1 implicates altered protein stability and function

Shah Kamal[1†*], Amanullah Amanullah[1†], Qingqing Wang[1], Najeeb Ullah[1], Gohar Mushtaq[2*], Muhammad Nasir Iqbal[3], and Mohammad Amjad Kamal[4,5,6,7,8]

[1]Jiangsu Key Laboratory for Biodiversity and Biotechnology, College of Life Sciences, Nanjing Normal University, Nanjing, China

[2]Department of Biochemistry, Center for Scientific Research, Faculty of Medicine, Idlib University, Idlib, Syria

[3]Department of Bioinformatics, Faculty of Biological and Chemical Sciences, The Islamia University of Bahawalpur, Pakistan

[4]Joint Laboratory of Artificial Intelligence for Critical Care Medicine, Department of Critical Care Medicine and Institutes for Systems Genetics, West China School of Nursing, Frontiers Science Center for Disease-related Molecular Network, West China Hospital, Sichuan University, Chengdu, China

[5]King Fahd Medical Research Center, King Abdulaziz University, Jeddah, Saudi Arabia

[6]Department of Pharmacy, Faculty of Health and Life Sciences, Daffodil International University, Birulia, Savar, Dhaka, Bangladesh

[7]Centre for Global Health Research, Saveetha Medical College and Hospital, Saveetha Institute of Medical and Technical Sciences, Chennai, Tamil Nadu, India

[8]Enzymoics, 7 Peterlee Place, Hebersham, NSW, Novel Global Community Educational Foundation, Australia

[†]*These authors contributed equally to this work.*

***Corresponding authors:**
Shah Kamal
(31183001@njnu.edu.cn)
Gohar Mushtaq
(dr.goher_mushtaq@idlib-university.com)

Citation: Kamal S, Amanullah A, Wang Q, *et al*. Bioinformatics analysis of missense mutations in CXCR1 implicates altered protein stability and function. *Tumor Discov*. 2024;3(1):2512. https://doi.org/10.36922/td.2512

Received: December 22, 2023
Accepted: February 21, 2024
Published Online: March 21, 2024

Copyright: © 2024 Author(s). This is an Open-Access article distributed under the terms of the Creative Commons Attribution License, permitting distribution, and reproduction in any medium, provided the original work is properly cited.

Publisher's Note: AccScience Publishing remains neutral with regard to jurisdictional claims in published maps and institutional affiliations.

Abstract

Human CXCR1 is a G-protein α subunit i (Gαi)-coupled receptor (GPCR) that plays an important role in promoting leukocyte recruitment and activation in inflammatory regions; thus, its genetic contribution to human disorders warrants further investigation. In this study, we investigated whether oncogenic missense mutations in CXCR1 would affect its activity and hinder its ability to interact with its ligand. This study utilized a bioinformatics approach and employed precise and thorough computational methods to gain insights into the molecular characteristics of mutated CXCR1 that are responsible for causing diseases. I-TASSER was used to construct a mutant model with the required mutations. Schrödinger's Desmond software was used to evaluate how mutations affect the stability and function of proteins. In this study, 299 CXCR1 missense mutations were examined; 53 of these were reported to be disease-causing, five of which were directly associated with cancer. The impact of the three cancer-causing mutations (N57D, R135C, and P302S) on protein stability and function was subsequently examined through computational analysis. Positions N57, R135, and P302 were determined to be highly conserved, and substitutions with aspartic acid (D), cysteine (C), and serine (S), respectively, could impair CXCR1 activity. Hence, our findings suggested that these mutations could alter CXCR1 ligand binding activity, lowering the risk of cancer and helping patients defend against pathogen invasion during a neutrophil-mediated innate immune response.

Keywords: CXCR1; Molecular dynamic simulation; Molecular modeling; G protein-coupled receptors

1. Introduction

CXCR1 is a rhodopsin-like (class A) G protein-coupled receptor (GPCR) that plays a crucial role in cellular signaling and is being investigated as a potential drug receptor due to its involvement in various physiological processes.[1,2] Rhodopsin is commonly used as a standard structure for mimicking GPCRs, and many rhodopsin structures have been characterized in protein databases (PDBs).[3] CXCR1 is one of two receptors that has a strong binding affinity for the CXC chemokine interleukin-8 (IL-8).[4] IL-8 is also known to regulate inflammatory and immune responses and has been linked to various diseases, including cancer.[5] On exposure to inflammatory stimuli, the chemokine IL-8 binds to the extracellular (EC) region of CXCR1.[6] Despite the physiological importance of CXCR1, the underlying molecular mechanism of its signal transduction pathway is poorly understood, primarily due to the limited availability of its structural information.[7]

GPCRs, including CXCR1, typically consist of seven transmembrane (TM) helices, four EC regions (comprising the N-terminal and three interhelical loops), and four intracellular (IC) regions (including the C-terminal and three interhelical loops).[8] Among the seven TM helices, TM3 and TM6 are regarded as pivotal elements responsible for activating switches in GPCRs, and these regions play a critical role in the transition from a partially active state to a fully activated state, particularly in the interactions between G proteins and receptors.[8,9] Crystal structures of the human adenosine A2A receptor bound to rhodopsin and agonists indicate that GPCR activation is induced by the disruption of crucial interhelical interactions.[10] Activation involves the rotation of the TM3 and TM6 domains, thereby altering the conformational structure of the receptor's G protein-interacting cytoplasmic loops to expose previously masked G protein-binding sites on the IC loops.[11] Recent advances in GPCR structural determination have studied the molecular mechanisms of GPCR activation and activity in various cellular processes, such as hormone signaling and neurotransmission.[12] The techniques used to study GPCRs involve several modifications, including making changes to the receptors themselves, adding small molecules to stabilize them, and using specialized lipid mixtures to form crystals that can be analyzed.[13,14] Activation of CXCR1 requires the involvement of both amino-terminal residues and EC loops. In this process, GPCR IC loops play a crucial role in facilitating interactions with G proteins during signaling.[4,15]

According to experimental research, charge significantly influences the interaction of CXCR1 with IL-8/CXCL8, and charged residues in the third and fourth EC loops are essential for this association.[16] Nuclear magnetic resonance spectroscopy (NMR) investigations have also reported that residues after the CXC sequence and those in the core β sheet of IL-8/CXCL8 bind directly to the N-terminus of CXCR1.[17] The ELR motif of the CXC chemokine on the N-terminus of IL-8/CXCL8 plays a role in the interaction of the chemokine with CXCR1.[18] Swapping the IC C-terminal regions consisting of 60 amino acids between CXCR1 and CXCR2 reportedly reversed the antagonistic effects of these receptors.[19] Further studies have demonstrated that the relative antagonistic effects of CXCR1 on CXCR2 were determined by a single amino acid residue: lysine 320 in CXCR2 and asparagine 311 in CXCR1.[19] The charged amino acids play a crucial role in maintaining the local structural stability required for binding in CXCR1, and mutating them disrupts this stability and prevents binding.[6] The mutations that were studied involved charged amino acids in various regions of the CXCR1 receptor, including TM helices and EC loops.[20] These mutations were predicted to alter the local structure of the receptor and potentially affect its ability to bind to other molecules. Specifically, the mutations were predicted to disrupt ion pairs, and oppositely charged amino acids would form bonds that can affect the receptor's capacity to maintain a stable structure in these regions.[21]

Identifying deleterious mutations and predicting the effects of missense mutations on protein structure and function have become important applications of computational analysis.[22] This approach can aid in the design of new drugs and therapies for treating various genetic diseases; for this reason, in the present study, we evaluated the possible consequences of mutations in the various CXCR1 domains that can affect protein function and interactions with ligands. To categorize harmful mutations, we initially used several computational algorithms, including Meta-SNP,[23] PMut,[24] and PROVEAN.[25] We also utilized the FATHMM server to detect specific genetic variants associated with carcinogenesis within disease-causing mutations.[26] Moreover, we employed mCSM,[27] SDM,[28] and DUET[29] to predict the impact of these mutations on the structure and stability of the corresponding proteins. The I-TASSER server was used to create a mutation model with the necessary missense mutation, and Schrödinger's Desmond 3D modeling software was used to explore the structural changes that affect the stability and function of the CXCR1 protein.

2. Methods

2.1. Collection of datasets

To obtain information on CXCR1 missense mutations, the study collected data from Ensembl (release 109)[30] and the Universal Protein Resource Knowledgebase (UniProtKB),

including sequence information in FASTA format (UniProt ID: P25024) from the National Centre for Biological Information (NCBI).[31,32] The structural information of CXCR1 was obtained from the Protein Data Bank (PDB) (http://www.rcsb.org/) with PDB ID: 2LNL.[33]

2.2. Computer-assisted pathogenicity analysis of the mutations

Computational techniques play a vital role in assessing the effect of mutations on proteins and distinguishing between deleterious and benign single-nucleotide variations. This capability is crucial for accurately distinguishing the impact of genetic alterations on protein function, facilitating the identification of disease-causing mutations. Meta-SNPs are web-based tools (http://snps.biofold.org/meta-snp/) that employ multiple predictive algorithms to assess the potentially detrimental effects of protein mutations.[23] The tool integrates other prediction methods, such as SNAP,[34] PhD-SNP, PANTHER,[35] and SIFT,[36] into the system, making it one of the most powerful tools for predicting the impact of mutations on protein function. Meta-SNPs utilize a random forest algorithm consisting of 100 decision trees implemented through the WEKA library.[37] This algorithm was trained on the SV-2009 dataset using a rigorous 20-fold cross-validation methodology.[23] The output of this predictor is a probability score indicating the likelihood of a mutation causing a disease, with scores <0.5 indicating a greater likelihood of the mutation being pathogenic.[38]

The PROVEAN web server applies an alignment-created scoring methodology to determine whether an amino acid replacement affects a protein's biological function.[25] In this approach, mutations with final scores <2.5 were considered harmful. The web server can be accessed at (http://provean.jcvi.org/seq_submit.php).[39]

2.3. Analysis of protein stability

Mutations in a protein can modify its stability and free energy, wherein the difference in free energy (ΔΔG) between the mutated (ΔGm) and wild-type (ΔGw) proteins reflects the effect of mutation on protein stability.[28,40] A negative ΔΔG value represents a destabilizing mutation, while a positive ΔΔG value indicates a stabilizing mutation.[28,40] Several computational approaches, including mCSM, SDM, and DUET, were used to determine the effect of mutations on protein stability.[28]

SDM2 (http://marid.bioc.cam.ac.uk/sdm2) is a computational method designed to predict the quantitative impact of mutations on protein stability.[28,41] SDM2 analyses the variation in potential amino acid substitutions within a specific structural environment tolerated by homologous proteins with known 3D structures.[42] This information is used to generate substitution probability tables, which are subsequently employed to estimate the predicted impact of a mutation on protein stability.[41]

The mCSM computational approach (http://structure.bioc.cam.ac.uk/mcsm)[27] was specifically designed to predict the effects of missense mutations on both protein stability and interactions with its corresponding ligands.[22] This prediction technique utilizes graph-based signatures to capture atom distance patterns, enabling precise evaluations of the effect of mutations on protein stability and interactions. In detail, mCSM encodes spatial relationships between atoms and provides insights into the structural consequences of genetic variations at the atomic level.[43] These signatures enable the mapping of the protein residue environment and the training of predictive models. In addition to evaluating the effect of mutations on protein stability, mCSM also takes into account possible interactions with proteins and nucleic acids. Therefore, the mCSM computational approach can provide valuable insights into how mutations might contribute to the development of various diseases.[44]

DUET (http://structure.bioc.cam.ac.uk/duet)[29] is a computational method that combines two prediction approaches, mCSM and SDM, to accurately predict the effects of missense mutations on protein stability.[29] The predictions generated by these methods are combined using support vector machines (SVMs) that have been trained with sequential minimal optimization.[45] By integrating these methods, DUET can produce a consensus prediction, offering a reliable and optimized approach for accurately predicting the effects of mutations on protein stability.[29]

2.4. Evaluation of cancer-related mutations through the FATHMM server

We utilized the FATHMM server (http://fathmm.biocompute.org.uk/cancer.html) to assess the relevance of harmful mutations to cancer. This web-based tool provides predictions that enable differentiation between cancer-causing mutations and other nonpathogenic germline polymorphisms.[46] We accurately assessed the potential role of deleterious mutations in cancer development, enhancing our understanding of the genetic basis of cancer and facilitating the identification of clinically significant mutations.[26]

2.5. Protein structure modeling of the mutation site

To construct a mutant model of CXCR1 with targeted mutations (N57D, R135C, and P302S), the crystal structure of the native protein was downloaded from PDB, and the

I-TASSER server was subsequently used with a multiple threading approach to construct the desired mutant model.[47]

2.6. Evaluation of the quality of the protein model

The CXCR1 protein is a complex molecule composed of amino acids, and its function is associated with its specific 3D structure. Understanding the structure of a protein can provide insights into its function, interactions with other molecules, and potential roles in biological processes, and the CXCR1 protein is a chemokine receptor involved in the immune system and inflammation.[48] The CXCR1 mutant and native protein models were designed through the I-TASSER server[47] and subsequently subjected to quality validation using the RAMPAGE server (https://servicesn.mbi.ucla.edu/PROCHECK).[49] The quality validation involved analyzing the stereochemical features of the models, including bond lengths, bond angles, and torsion angles, thereby ensuring that the protein models have a geometrically and chemically plausible conformation. Significant deviations in the model's stereochemical features from expected values may indicate errors in the model.[49] In addition, the protein models were compared against experimental data to evaluate their arrangement with known structural properties. This comparison aimed to validate the accuracy of the predicted models by assessing how well they aligned with the actual structure of the CXCR1 protein.

The quality of the protein models refers to their accuracy and reliability in representing the true 3D structure of the CXCR1 protein. The validation process ensures that the models have appropriate stereochemical features and are consistent with the experimental data, enhancing confidence in their utility for further research and analysis.[50] Using the RAMPAGE server, we ensured the reliability of the mutant and normal protein models by checking the stereochemical quality of the protein structure by analyzing the residue-by-residue geometry and overall structural geometry.

2.7. Molecular dynamics simulation

Molecular dynamics simulation (MDS) is a computational technique that simulates the movements and interactions of atoms and molecules over time. It provides a dynamic, detailed view of how biological molecules, such as proteins, behave at the atomic level for studying molecular structures, dynamics, and interactions, offering insights that are often challenging to obtain through experimental methods.[51] In MDS, a protein model is a 3D representation of the protein's structure that is used as the starting point for simulations.[51] The quality of the model is crucial for obtaining accurate simulation results.[52] Key factors for a high-quality protein model include an accurate representation of the native structure, compatibility with a suitable force field, inclusion of the surrounding solvent and relevant environmental factors, and the ability to undergo post-simulation analysis.[53] Ensuring these aspects enhances the reliability and biological relevance of insights gained from MDS.

The mutant and normal model structures with the highest I-TASSER score, indicating their favorable conformational arrangement, were chosen for subsequent investigation and analysis.[47] To investigate the effect of the identified mutations on the structure of CXCR1 at the mechanistic level, we conducted an MDS using Schrödinger's Desmond software.[54,55] Specifically, we analyzed the effects of the N57D, R135C, and P302S mutations on the protein structure over a simulation period of 100 ns.[56] As a critical first step, protein docking was performed before MDS, predicting the static binding position of the molecule at the active site of the protein and providing important information for the subsequent analysis of the protein's structure and function during the simulation.[55] MDS typically utilizes Newton's classical equation of motion to simulate the movements of atoms over time, providing predictions of ligand-binding status in various physiological environments.[51] By modeling the behavior of individual particles based on physical laws, MDS can provide valuable insights into the dynamic behavior and stability of proteins under diverse conditions.[54] Maestro's Protein Preparation Wizard was used to optimize, minimize, and replace missing residues in the CXCR1 receptor protein. In addition, the MDS system was constructed using the System Builder tool, where the TIP3P (Intermolecular Interaction Potential 3 Points Transferable) solvent model with 300 K temperature, 1 atm pressure, and OPLS_2005 force field was applied.[57] The models were neutralized by adding counterions and 0.15 M sodium chloride and subsequently used to simulate physiological conditions. Before simulation, the models were equilibrated, and trajectories were saved for analysis every 100 ps.[58] The stability of the simulations was assessed by calculating the root mean square deviation (RMSD) and root mean square fluctuation (RMSF) of the proteins during the simulation period.[58]

RMSD determines the average change in the distance of a set of atoms concerning a reference frame, and it is computed for each frame of trajectory.[59] The RMSD for frame x is:

$$\mathrm{RMSD}_{\mathrm{X}} = \sqrt{1/N\sum_{i=1}^{n}\left(\mathrm{r`i}(35)\right) - ri(tref))^2} \qquad \text{(I)}$$

Where N is the number of atoms in atom selection; *tref* is the reference time (typically, the first frame is used as

a reference, and time is considered as t = 0); and r is the position of selected atoms in frame x after superposition with the reference frame (frame x being recorded at time tx). The procedure was repeated for each frame in the simulation trajectory.[59]

RMSF is useful for characterizing local changes in the protein chain.[54] The RMSF for residue i is:

$$\mathrm{RMSF}_i = \sqrt{1/T\sum_{t=1}^{T} < \left(r`i(\mathrm{t})\right) - ri(tref))^2 >} \quad \text{(II)}$$

Where T is the flight path time over which the RMSF is calculated; *tref* is the reference time; *ri* is the position of residue I; r is the position of the atoms in residue I after an overlay with the reference; and the angle brackets indicate that the mean squared distance is taken over the selection of the atoms in residue I.[54]

2.8. Analysis of secondary structure changes in CXCR1 proteins

The Database of Secondary Structure in Proteins tool utilizes hydrogen bonding and other secondary structure markers to categorize protein residues and examine alterations in secondary structure patterns between wild-type and mutant CXCR1 proteins.[60] The resulting secondary structure patterns were plotted for comparison.

3. Results

This study demonstrated that missense mutations in the CXCR1 gene significantly affected the molecular structure, stability, and function of the resulting protein. This finding suggested that the altered protein could be dysfunctional and contribute to the development or progression of disease. The study utilized advanced computational methods to screen for protein stability, cancer-causing mutations, and pathogenicity.

3.1. Retrieving the dataset of missense mutations

To explore the potential effects of CXCR1 gene mutations on protein function, we acquired a comprehensive list of 299 mutations (Table S1) from a publicly available database. These mutations are distributed throughout different coding regions of the gene, allowing for a comprehensive assessment of the potential impact on protein functionality.

3.2. Analysis of missense mutations

The importance of missense mutations in amino acids can be used to assess the pathogenic implications of these mutations. PMut, PROVEAN, and Meta-SNPs (PANTHER, PhD-SNP, SIFT, and SNAP) were used to investigate the 299 missense mutations. We found that 53 mutations in CXCR1 could cause harm and disease, and these mutations were located across multiple domains of the protein (Table 1).

3.3. Prediction of the impact of mutation on CXCR1 protein stability

Three algorithms, mCSM, SDM, and DUET, were used to predict the 299 mutations and their impact on protein stability. mCSM predicted that 19 mutations would strongly destabilize protein stability, SDM predicted that 183 mutations would reduce CXCR1 protein stability, and DUET predicted that 240 amino acids would affect the stability of the CXCR1 protein (Table 2).

3.4. Identification of potential carcinogenic mutations in CXCR1

In CXCR1, 299 mutations were identified using the FATHMM server to determine their potential role in carcinogenesis. The analysis revealed five specific carcinogenic mutations (N57D, R135C, R135H, R135L, and P302S) (Table 3), and these mutations were located across different regions of CXCR1.

3.5. Conservation analysis

From the five identified carcinogenic mutations, three mutations, N57D, R135C, and P302S, were selected for further analysis. This analysis utilized the ConSurf server tool to examine the conservation and location of these three mutations.[61] The results indicated high conservation levels at these locations, with a score of 9 on the scale presented in Figure 1A-C. Based on these findings, we subsequently investigated the impact of these three mutations on protein stability and function through simulated computational analysis.

3.6. Selection of the mutant CXCR1 structure

The control model for the native protein was the 3D structure of CXCR1 (PDB ID 2LNL).[62] The I-TASSER server was used to locate template proteins with comparable folds from the PDB database and construct 10,000 conformations (decoys) from a mutant sequence.[63] I-TASSER utilized the SPICKER tool to cluster the generated conformations by performing pairwise structural alignments.[64] This process grouped similar conformations, enabling a more organized analysis of the protein structures. Consequently, five separate clusters emerged, each having a large number of models with identical structures. I-TASSER then selected a representative model from each of these clusters to construct five final models that best represented the varied conformation predictions.[64] The first model was selected for further investigation because it had the greatest confidence level (C-score).[47] Ramachandran plots were

Table 1. Predicted deleterious CXCR1 mutations using computational tools

Serial number	Mutants	Computational tool													
		PANTHER		PhD-SNP		SIFT		SNAP		Meta-SNP		PMut		PROVEAN	
		Prediction	Score	Prediction	Score	Prediction	Score	Prediction	Score	Prediction	Score	Prediction	Score	Prediction	Score
38	Y46C	Harmful	0.824	Harmful	0.916	Harmful	0.02	Harmful	0.75	Harmful	0.843	Harmful	0.77	Harmful	−7.852
39	V49G	Harmful	0.599	Harmful	0.852	Harmful	0	Harmful	0.665	Harmful	0.764	Harmful	0.9	Harmful	−6.114
42	L51P	Harmful	0.801	Harmful	0.873	Harmful	0.04	Harmful	0.72	Harmful	0.802	Harmful	0.71	Harmful	−5.374
43	L52Q	Harmful	0.805	Harmful	0.726	Harmful	0.01	Harmful	0.615	Harmful	0.74	Harmful	0.9	Harmful	−4.576
45	N57D	Harmful	0.976	Harmful	0.807	Harmful	0	Harmful	0.85	Harmful	0.886	Harmful	0.9	Harmful	−4.449
47	L59P	Harmful	0.84	Harmful	0.862	Harmful	0	Harmful	0.76	Harmful	0.835	Harmful	0.69	Harmful	−5.697
70	L78P	Harmful	0.802	Harmful	0.874	Harmful	0	Harmful	0.76	Harmful	0.838	Harmful	0.9	Harmful	−6.065
73	A82V	Harmful	0.692	Harmful	0.805	Harmful	0.04	Harmful	0.58	Harmful	0.568	Harmful	0.56	Harmful	−3.302
75	D85N	Harmful	0.702	Harmful	0.814	Harmful	0.03	Harmful	0.76	Harmful	0.64	Harmful	0.54	Harmful	−3.604
79	T91I	Harmful	0.611	Harmful	0.827	Harmful	0.03	Harmful	0.64	Harmful	0.577	Harmful	0.58	Harmful	−4.447
81	P93S	Harmful	0.99	Harmful	0.874	Harmful	0	Harmful	0.75	Harmful	0.847	Harmful	0.91	Harmful	−7.124
82	P93T	Harmful	0.992	Harmful	0.838	Harmful	0	Harmful	0.75	Harmful	0.852	Harmful	0.91	Harmful	−7.135
83	P93H	Harmful	0.996	Harmful	0.894	Harmful	0	Harmful	0.83	Harmful	0.89	Harmful	0.91	Harmful	−8.016
89	W103R	Harmful	0.994	Harmful	0.958	Harmful	0	Harmful	0.885	Harmful	0.905	Harmful	0.91	Harmful	−12.088
99	C110W	Harmful	0.999	Harmful	0.962	Harmful	0	Harmful	0.87	Harmful	0.947	Harmful	0.91	Harmful	−9.933
100	K111E	Harmful	0.973	Harmful	0.892	Harmful	0.01	Harmful	0.74	Harmful	0.787	Harmful	0.91	Harmful	−3.612
106	Y122H	Harmful	0.584	Harmful	0.797	Harmful	0.02	Harmful	0.75	Harmful	0.634	Harmful	0.69	Harmful	−3.515
107	G124D	Harmful	0.552	Harmful	0.865	Harmful	0.03	Harmful	0.725	Harmful	0.754	Harmful	0.81	Harmful	−4.345
109	L127P	Harmful	0.965	Harmful	0.879	Harmful	0.01	Harmful	0.74	Harmful	0.739	Harmful	0.91	Harmful	−5.763
111	I131T	Harmful	0.898	Harmful	0.671	Harmful	0	Harmful	0.665	Harmful	0.715	Harmful	0.91	Harmful	−4.461
113	S132N	Harmful	0.746	Harmful	0.773	Harmful	0.02	Harmful	0.635	Harmful	0.6	Harmful	0.6	Harmful	−2.684
115	D134V	Harmful	0.973	Harmful	0.934	Harmful	0.02	Harmful	0.73	Harmful	0.728	Harmful	0.85	Harmful	−7.819
116	D134G	Harmful	0.923	Harmful	0.919	Harmful	0	Harmful	0.755	Harmful	0.725	Harmful	0.91	Harmful	−5.796
117	D134E	Harmful	0.861	Harmful	0.859	Harmful	0.05	Harmful	0.68	Harmful	0.65	Harmful	0.84	Harmful	−3.479
118	R135C	Harmful	0.996	Harmful	0.898	Harmful	0.01	Harmful	0.775	Harmful	0.834	Harmful	0.91	Harmful	−6.491
119	R135L	Harmful	0.99	Harmful	0.947	Harmful	0	Harmful	0.78	Harmful	0.779	Harmful	0.91	Harmful	−5.963
120	R135H	Harmful	0.992	Harmful	0.876	Harmful	0	Harmful	0.81	Harmful	0.781	Harmful	0.89	Harmful	−4.307
122	I139T	Harmful	0.909	Harmful	0.61	Harmful	0.05	Harmful	0.59	Harmful	0.627	Harmful	0.69	Harmful	−4.734
123	V140F	Harmful	0.929	Harmful	0.866	Harmful	0.04	Harmful	0.575	Harmful	0.773	Harmful	0.74	Harmful	−4.834
136	C157F	Harmful	0.981	Harmful	0.838	Harmful	0.04	Harmful	0.705	Harmful	0.85	Harmful	0.9	Harmful	−9.54

(Cont'd...)

Table 1. *(Continued)*

Serial number	Mutants	Computational tool													
		PANTHER		PhD-SNP		SIFT		SNAP		Meta-SNP		PMut		PROVEAN	
		Prediction	Score	Prediction	Score	Prediction	Score	Prediction	Score	Prediction	Score	Prediction	Score	Prediction	Score
139	W161L	Harmful	0.997	Harmful	0.857	Harmful	0.03	Harmful	0.78	Harmful	0.824	Harmful	0.9	Harmful	−11.781
140	W161C	Harmful	0.998	Harmful	0.912	Harmful	0.01	Harmful	0.8	Harmful	0.831	Harmful	0.9	Harmful	−11.797
142	S164F	Harmful	0.88	Harmful	0.807	Harmful	0	Harmful	0.715	Harmful	0.778	Harmful	0.9	Harmful	−4.409
146	P170T	Harmful	0.776	Harmful	0.819	Harmful	0.01	Harmful	0.71	Harmful	0.689	Harmful	0.86	Harmful	−6.798
147	P170L	Harmful	0.822	Harmful	0.891	Harmful	0.04	Harmful	0.63	Harmful	0.679	Harmful	0.87	Harmful	−8.641
160	C187Y	Harmful	0.993	Harmful	0.869	Harmful	0.02	Harmful	0.88	Harmful	0.902	Harmful	0.9	Harmful	−7.963
183	F211V	Harmful	0.981	Harmful	0.901	Harmful	0.01	Harmful	0.73	Harmful	0.844	Harmful	0.9	Harmful	−6.653
185	P214L	Harmful	0.994	Harmful	0.903	Harmful	0.01	Harmful	0.665	Harmful	0.853	Harmful	0.9	Harmful	−9.694
189	Y222C	Harmful	0.998	Harmful	0.888	Harmful	0.02	Harmful	0.63	Harmful	0.852	Harmful	0.91	Harmful	−7.669
193	T225P	Harmful	0.683	Harmful	0.846	Harmful	0.01	Harmful	0.67	Harmful	0.806	Harmful	0.9	Harmful	−4.677
214	I244N	Harmful	0.82	Harmful	0.865	Harmful	0	Harmful	0.645	Harmful	0.75	Harmful	0.9	Harmful	−6.676
215	I244F	Harmful	0.627	Harmful	0.819	Harmful	0.01	Harmful	0.655	Harmful	0.658	Harmful	0.84	Harmful	−3.868
219	P257S	Harmful	1	Harmful	0.853	Harmful	0	Harmful	0.76	Harmful	0.908	Harmful	0.9	Harmful	−7.691
254	L293P	Harmful	0.843	Harmful	0.877	Harmful	0	Harmful	0.825	Harmful	0.869	Harmful	0.91	Harmful	−6.313
257	C299F	Harmful	0.976	Harmful	0.961	Harmful	0.02	Harmful	0.74	Harmful	0.849	Harmful	0.85	Harmful	−8.438
258	P302S	Harmful	1	Harmful	0.873	Harmful	0	Harmful	0.76	Harmful	0.938	Harmful	0.91	Harmful	−7.503
259	I304N	Harmful	0.776	Harmful	0.845	Harmful	0	Harmful	0.675	Harmful	0.773	Harmful	0.91	Harmful	−5.543
262	F312S	Harmful	0.998	Harmful	0.914	Harmful	0	Harmful	0.69	Harmful	0.876	Harmful	0.91	Harmful	−7.503
263	F312I	Harmful	0.998	Harmful	0.909	Harmful	0.03	Harmful	0.595	Harmful	0.861	Harmful	0.72	Harmful	−5.627
265	R313H	Harmful	0.566	Harmful	0.862	Harmful	0.03	Harmful	0.565	Harmful	0.722	Harmful	0.75	Harmful	−4.288
267	R313C	Harmful	0.795	Harmful	0.927	Harmful	0	Harmful	0.73	Harmful	0.825	Harmful	0.82	Harmful	−6.834
272	I319N	Harmful	0.855	Harmful	0.611	Harmful	0.04	Harmful	0.555	Harmful	0.701	Harmful	0.9	Harmful	−4.91
273	L320P	Harmful	0.773	Harmful	0.889	Harmful	0.01	Harmful	0.755	Harmful	0.828	Harmful	0.69	Harmful	−5.456

Table 2. Predicted CXCR1 mutations that decrease or damage protein stability using computational servers

Serial number	Computational server					
	SDM		mCSM		DUET	
	ΔΔG	Prediction of protein stability	ΔΔG	Prediction of protein stability	ΔΔG	Prediction of protein stability
1	0	Enhance	−0.8	Damaging	−0.49	Damaging
2	0	Enhance	−0.989	Damaging	−0.691	Damaging
4	0	Enhance	−0.623	Damaging	−0.253	Damaging
5	0	Enhance	−0.8	Damaging	−0.49	Damaging
6	−1.29	Decrease	−0.88	Damaging	−0.959	Damaging
7	0.02	Enhance	−0.126	Damaging	0.101	Stabilizing
8	−0.05	Decrease	−1.091	Damaging	−0.676	Damaging
9	−0.42	Decrease	−2.522	Highly damaging	−2.139	Damaging
10	−0.59	Decrease	−2.751	Highly damaging	−2.931	Damaging
11	−0.8	Decrease	−3.373	Highly damaging	−3.693	Damaging
12	−0.46	Decrease	−0.337	Damaging	−0.444	Damaging
13	−0.25	Decrease	−0.635	Damaging	−0.508	Damaging
14	−0.18	Decrease	−0.387	Damaging	−0.031	Damaging
15	0.1	Enhance	−0.375	Damaging	−0.062	Damaging
16	0.78	Enhance	−0.28	Damaging	0.24	Stabilizing
17	−0.18	Decrease	−0.543	Damaging	−0.292	Damaging
18	−0.43	Decrease	−0.295	Damaging	−0.011	Damaging
19	−0.11	Decrease	−0.573	Damaging	−0.274	Damaging
20	−0.11	Decrease	0.093	Stabilizing	0.172	Stabilizing
21	3.78	Enhance	−0.42	Damaging	0.437	Stabilizing
22	1.18	Enhance	−0.265	Damaging	0.111	Stabilizing
24	0.78	Enhance	−0.297	Damaging	0.296	Stabilizing
25	−0.29	Decrease	−0.623	Damaging	−0.456	Damaging
26	0.67	Enhance	−0.531	Damaging	−0.09	Damaging
27	0.25	Enhance	−0.6	Damaging	−0.151	Damaging
28	−0.5	Decrease	−0.125	Damaging	0.139	Stabilizing
29	0.34	Enhance	−0.048	Damaging	0.468	Stabilizing
30	−0.98	Decrease	−0.491	Damaging	−0.407	Damaging
31	−0.63	Decrease	−0.814	Damaging	−0.846	Damaging
32	0.36	Enhance	−0.299	Damaging	0.192	Stabilizing
34	0.23	Enhance	−0.398	Damaging	0.045	Stabilizing
35	−0.65	Decrease	−0.231	Damaging	0.174	Stabilizing
36	0.09	Enhance	−0.598	Damaging	−0.221	Damaging
37	−2.05	Decrease	−1.013	Damaging	−1.122	Damaging
38	−1.01	Decrease	−1.571	Damaging	−1.411	Damaging
39	−2.5	Decrease	−2.547	Highly damaging	−2.932	Damaging
40	0.64	Enhance	−1.12	Damaging	−0.806	Damaging
41	0.04	Enhance	−1.266	Damaging	−1.102	Damaging
42	−2.23	Decrease	−0.564	Damaging	−0.569	Damaging
43	−2.23	Decrease	−1.29	Damaging	−1.158	Damaging

(Cont'd...)

Table 2. ***(Continued)***

Serial number	Computational server					
	SDM		mCSM		DUET	
	ΔΔG	Prediction of protein stability	ΔΔG	Prediction of protein stability	ΔΔG	Prediction of protein stability
44	−0.67	Decrease	−1.492	Damaging	−1.302	Damaging
45	−0.62	Decrease	−2.418	Highly damaging	−2.346	Damaging
46	0.43	Enhance	−0.838	Damaging	−0.466	Damaging
47	−2.23	Decrease	−0.799	Damaging	−1.093	Damaging
48	−0.15	Decrease	−1.34	Damaging	−0.823	Damaging
49	0.11	Enhance	−0.995	Damaging	−0.382	Damaging
50	−2.23	Decrease	−0.793	Damaging	−1.086	Damaging
51	−0.2	Decrease	0.141	Stabilizing	0.532	Stabilizing
52	−1.5	Decrease	−1.928	Damaging	−2.145	Damaging
53	−0.35	Decrease	−1.305	Damaging	−1.083	Damaging
54	−0.91	Decrease	−0.095	Damaging	0.13	Stabilizing
55	−1.51	Decrease	−0.661	Damaging	−0.629	Damaging
56	0.22	Enhance	−0.199	Damaging	0.255	Stabilizing
57	−1.21	Decrease	−0.267	Damaging	−0.138	Damaging
58	−0.3	Decrease	−0.47	Damaging	−0.246	Damaging
59	−0.4	Decrease	−0.633	Damaging	−0.48	Damaging
60	−0.33	Decrease	−0.293	Damaging	−0.291	Damaging
61	0.09	Enhance	−0.657	Damaging	−0.537	Damaging
62	−0.59	Decrease	−0.984	Damaging	−0.909	Damaging
63	0.35	Enhance	−0.726	Damaging	−0.256	Damaging
64	−0.01	Decrease	−1.113	Damaging	−0.965	Damaging
65	−0.17	Decrease	−0.79	Damaging	−0.529	Damaging
66	−0.97	Decrease	−1.319	Damaging	−1.476	Damaging
67	−0.2	Decrease	−0.734	Damaging	−0.402	Damaging
68	0.11	Enhance	−1.439	Damaging	−0.979	Damaging
69	−1.35	Decrease	−2.371	Highly damaging	−2.214	Damaging
70	−2.75	Decrease	−0.963	Damaging	−1.327	Damaging
71	−0.52	Decrease	−0.638	Damaging	−0.101	Damaging
72	0.12	Enhance	−1.215	Damaging	−0.799	Damaging
73	−0.85	Decrease	−0.668	Damaging	−0.546	Damaging
74	−3.32	Decrease	−2.982	Highly damaging	−3.32	Damaging
75	0.57	Enhance	−1.063	Damaging	−0.659	Damaging
76	−0.37	Decrease	−0.994	Damaging	−0.708	Damaging
77	−1.41	Decrease	−1.807	Damaging	−1.933	Damaging
78	−2.61	Decrease	−1.29	Damaging	−1.518	Damaging
80	−1.48	Decrease	−1.249	Damaging	−1.528	Damaging
81	1.62	Enhance	−1.559	Damaging	−1.017	Damaging
82	0.34	Enhance	−1.298	Damaging	−0.848	Damaging
83	1.06	Enhance	−1.306	Damaging	−0.776	Damaging
84	−2.83	Decrease	−2.726	Highly damaging	−2.636	Damaging

(Cont'd...)

Table 2. *(Continued)*

Serial number	Computational server					
	SDM		mCSM		DUET	
	ΔΔG	Prediction of protein stability	ΔΔG	Prediction of protein stability	ΔΔG	Prediction of protein stability
85	−1.49	Decrease	−1.472	Damaging	−1.575	Damaging
86	−1.53	Decrease	−1.293	Damaging	−1.237	Damaging
87	0.65	Enhance	−0.161	Damaging	0.297	Stabilizing
88	−2.65	Decrease	−1.377	Damaging	−1.674	Damaging
89	−0.4	Decrease	−1.656	Damaging	−1.308	Damaging
90	−0.22	Decrease	−1.243	Damaging	−1.164	Damaging
91	−0.03	Decrease	−0.151	Damaging	0.239	Stabilizing
92	−1.33	Decrease	−0.923	Damaging	−0.83	Damaging
93	−0.65	Decrease	−1.619	Damaging	−1.655	Damaging
94	0.37	Enhance	−1.002	Damaging	−0.604	Damaging
95	−1.47	Decrease	−0.408	Damaging	−0.546	Damaging
96	0.64	Enhance	−0.62	Damaging	−0.322	Damaging
97	0.47	Enhance	−0.349	Damaging	0.008	Stabilizing
98	0.64	Enhance	−0.62	Damaging	−0.322	Damaging
99	−2.1	Decrease	−1.016	Damaging	−1.246	Damaging
100	0.09	Enhance	−1.65	Damaging	−1.233	Damaging
101	0.07	Enhance	−1.903	Damaging	−1.582	Damaging
102	0.18	Enhance	−1.353	Damaging	−1.029	Damaging
103	0.16	Enhance	−0.107	Damaging	0.101	Stabilizing
104	−1.65	Decrease	−0.904	Damaging	−1.041	Damaging
105	−0.53	Decrease	−1.465	Damaging	−1.453	Damaging
106	0.12	Enhance	−0.56	Damaging	−0.459	Damaging
107	−1.31	Decrease	−1.67	Damaging	−1.548	Damaging
108	0.78	Enhance	−1.844	Damaging	−1.726	Damaging
109	−2.55	Decrease	−1.164	Damaging	−1.541	Damaging
110	−4.41	Decrease	−1.686	Damaging	−2.378	Damaging
111	−2.05	Decrease	−1.481	Damaging	−1.619	Damaging
112	−3.12	Decrease	−2.55	Highly damaging	−2.883	Damaging
113	−1.12	Decrease	−0.883	Damaging	−0.605	Damaging
114	0.06	Enhance	−1.291	Damaging	−1.084	Damaging
115	0.16	Enhance	−0.467	Damaging	−0.21	Damaging
117	−0.32	Decrease	−1.154	Damaging	−1.048	Damaging
118	1.25	Enhance	−0.593	Damaging	0.048	Stabilizing
119	−0.74	Decrease	−0.781	Damaging	−0.681	Damaging
120	0.3	Enhance	−0.047	Damaging	0.352	Stabilizing
121	−0.06	Decrease	−1.476	Damaging	−1.263	Damaging
122	−2.05	Decrease	−1.446	Damaging	−1.582	Damaging
123	−1.06	Decrease	−1.247	Damaging	−1.171	Damaging
124	−0.09	Decrease	−1.191	Damaging	−1.071	Damaging
125	−0.35	Decrease	−0.029	Damaging	−0.118	Damaging
126	−0.38	Decrease	−0.181	Damaging	−0.253	Damaging

(Cont'd...)

Table 2. *(Continued)*

Serial number	Computational server					
	SDM		mCSM		DUET	
	ΔΔG	Prediction of protein stability	ΔΔG	Prediction of protein stability	ΔΔG	Prediction of protein stability
127	0.19	Enhance	−1.058	Damaging	−0.982	Damaging
128	−0.33	Decrease	−0.244	Damaging	−0.312	Damaging
129	0.42	Enhance	−0.229	Damaging	0.08	Stabilizing
130	0.27	Enhance	−0.333	Damaging	−0.096	Damaging
131	−0.19	Decrease	−0.034	Damaging	0.08	Stabilizing
132	−1.02	Decrease	−1.125	Damaging	−1.246	Damaging
133	−0.71	Decrease	−0.389	Damaging	−0.304	Damaging
134	0.65	Enhance	1.207	Stabilizing	1.307	Stabilizing
135	−0.63	Decrease	−1.173	Damaging	−1.225	Damaging
136	−0.09	Decrease	−1.133	Damaging	−1.103	Damaging
137	−1.5	Decrease	−1.281	Damaging	−1.426	Damaging
138	−0.63	Decrease	−0.974	Damaging	−0.997	Damaging
139	0.16	Enhance	−0.175	Damaging	0.345	Stabilizing
140	0.23	Enhance	−1.909	Damaging	−1.398	Damaging
141	0.08	Enhance	−1.432	Damaging	−1.007	Damaging
142	−2.23	Decrease	−0.758	Damaging	−0.987	Damaging
143	−0.2	Decrease	−1.02	Damaging	−0.766	Damaging
144	0.49	Enhance	−1.088	Damaging	−0.526	Damaging
145	0.11	Enhance	−0.405	Damaging	0.211	Stabilizing
146	0.49	Enhance	−1.618	Damaging	−1.179	Damaging
147	0.83	Enhance	−1.285	Damaging	−0.702	Damaging
149	0.11	Enhance	−1.069	Damaging	−0.916	Damaging
150	−0.65	Decrease	−2.752	Highly damaging	−2.836	Damaging
151	−1.29	Decrease	−1.693	Damaging	−2.099	Damaging
152	0.19	Enhance	−1.548	Damaging	−1.28	Damaging
153	0.25	Enhance	−2.782	Highly damaging	−2.451	Damaging
154	0.1	Enhance	−1.463	Damaging	−1.226	Damaging
155	−1.43	Decrease	−1.591	Damaging	−1.665	Damaging
156	−0.62	Decrease	0.073	Stabilizing	0.073	Stabilizing
157	0.94	Enhance	−0.824	Damaging	−0.379	Damaging
158	0.74	Enhance	−0.654	Damaging	−0.285	Damaging
159	−1.13	Decrease	−0.654	Damaging	−1.941	Damaging
160	−1.09	Decrease	−0.594	Damaging	−0.426	Damaging
161	−0.87	Decrease	−1.035	Damaging	−1.078	Damaging
162	−0.13	Decrease	−0.78	Damaging	−0.518	Damaging
163	−1.04	Decrease	−1.811	Damaging	−1.633	Damaging
164	−0.48	Decrease	−1.084	Damaging	−0.889	Damaging
165	0.84	Enhance	−0.634	Damaging	−0.28	Damaging
166	0.5	Enhance	−0.254	Damaging	0.074	Stabilizing
167	0.33	Enhance	−0.455	Damaging	−0.561	Damaging
168	−3.33	Decrease	−1.864	Damaging	−2.165	Damaging

(Cont'd...)

Table 2. *(Continued)*

Serial number	Computational server					
	SDM		mCSM		DUET	
	ΔΔG	Prediction of protein stability	ΔΔG	Prediction of protein stability	ΔΔG	Prediction of protein stability
169	−1.16	Decrease	−0.462	Damaging	−0.005	Damaging
170	−2	Decrease	−1.04	Damaging	−1.504	Damaging
171	0.54	Enhance	−0.842	Damaging	−0.13	Damaging
172	−0.72	Decrease	−1.493	Damaging	−1.341	Damaging
173	0.84	Enhance	−1.165	Damaging	−0.552	Damaging
174	−2.59	Decrease	−2.779	Highly damaging	−3.094	Damaging
175	−0.55	Decrease	−0.853	Damaging	−0.801	Damaging
176	0.37	Enhance	−0.144	Damaging	0.025	Stabilizing
177	−0.8	Decrease	−1.71	Damaging	−1.572	Damaging
178	−1.5	Decrease	−1.578	Damaging	−1.435	Damaging
179	−2.11	Decrease	−1.044	Damaging	−1.096	Damaging
180	−0.35	Decrease	−0.933	Damaging	−0.892	Damaging
181	0.21	Enhance	−0.998	Damaging	−0.712	Damaging
182	0.1	Enhance	−1.409	Damaging	−1.197	Damaging
183	−2.05	Decrease	−0.47	Damaging	−0.695	Damaging
184	−2.67	Decrease	−0.991	Damaging	−1.342	Damaging
185	0.16	Enhance	−0.173	Damaging	0.098	Stabilizing
186	3.38	Enhance	−0.426	Damaging	0.61	Stabilizing
187	0.64	Enhance	−0.823	Damaging	−0.527	Damaging
188	0.35	Enhance	−0.51	Damaging	−0.027	Damaging
189	0.18	Enhance	−0.833	Damaging	−0.274	Damaging
190	−1.5	Decrease	−1.457	Damaging	−1.465	Damaging
191	1.07	Enhance	−0.772	Damaging	−0.327	Damaging
192	1.64	Enhance	−0.581	Damaging	0.173	Stabilizing
193	1.36	Enhance	−1.094	Damaging	−0.279	Damaging
194	−1.22	Decrease	−0.326	Damaging	−0.524	Damaging
195	−1.82	Decrease	−0.345	Damaging	−0.662	Damaging
196	−0.7	Decrease	−1.456	Damaging	−1.455	Damaging
197	−0.74	Decrease	−0.821	Damaging	−0.811	Damaging
198	−0.82	Decrease	−0.238	Damaging	−0.172	Damaging
199	0.64	Enhance	−0.865	Damaging	−0.547	Damaging
200	−0.67	Decrease	−0.378	Damaging	−0.295	Damaging
201	−0.35	Decrease	−0.688	Damaging	−0.568	Damaging
203	0.6	Enhance	−0.361	Damaging	0.179	Stabilizing
204	0.54	Enhance	0.267	Damaging	0.276	Stabilizing
205	−0.19	Decrease	0.832	Stabilizing	0.982	Stabilizing
206	0.72	Enhance	−0.394	Damaging	−0.021	Damaging
208	−0.48	Decrease	−0.79	Damaging	−0.732	Damaging
209	0.79	Enhance	−0.491	Damaging	−0.298	Damaging
210	−1.06	Decrease	−0.168	Damaging	−0.363	Damaging
211	−1.53	Decrease	−1.021	Damaging	−1.229	Damaging

(Cont'd...)

Table 2. *(Continued)*

Serial number	Computational server					
	SDM		mCSM		DUET	
	ΔΔG	Prediction of protein stability	ΔΔG	Prediction of protein stability	ΔΔG	Prediction of protein stability
212	−0.28	Decrease	−0.405	Damaging	−0.325	Damaging
213	−2.99	Decrease	−2.176	Highly damaging	−2.148	Damaging
214	−0.25	Decrease	−0.363	Damaging	0.047	Stabilizing
215	−0.86	Decrease	−1.782	Damaging	−1.638	Damaging
216	−0.3	Decrease	−1.239	Damaging	−1.197	Damaging
217	−0.84	Decrease	0.386	Stabilizing	0.671	Stabilizing
218	−0.18	Decrease	0.15	Stabilizing	0.529	Stabilizing
219	−0.53	Decrease	−0.361	Damaging	−0.323	Damaging
220	0.49	Enhance	−2.066	Highly damaging	−1.769	Damaging
221	−1.53	Decrease	−1.463	Damaging	−1.42	Damaging
222	0.03	Enhance	−1.458	Damaging	−0.939	Damaging
223	0.01	Enhance	−1.507	Damaging	−1.291	Damaging
224	−0.09	Decrease	−1.052	Damaging	−0.497	Damaging
225	−0.99	Decrease	−0.705	Damaging	−0.083	Damaging
226	0.13	Enhance	−1.026	Damaging	−0.7	Damaging
227	−0.43	Decrease	−0.757	Damaging	−0.397	Damaging
228	1.51	Enhance	−0.009	Damaging	0.775	Stabilizing
229	−0.44	Decrease	−0.52	Damaging	−0.301	Damaging
230	−0.45	Decrease	−0.405	Damaging	−0.379	Damaging
231	0.04	Enhance	−1.163	Damaging	−0.919	Damaging
232	−0.61	Decrease	−0.787	Damaging	−0.67	Damaging
233	0.09	Enhance	−0.482	Damaging	−0.088	Damaging
234	−0.15	Decrease	−0.328	Damaging	0.074	Stabilizing
235	−1.01	Decrease	0.263	Stabilizing	0.474	Stabilizing
236	−2.54	Decrease	−0.193	Damaging	−0.826	Damaging
237	−1.1	Decrease	−1.393	Damaging	−1.484	Damaging
238	−0.87	Decrease	−0.582	Damaging	−0.543	Damaging
239	−0.65	Decrease	−0.863	Damaging	−0.775	Damaging
240	0.08	Enhance	−0.095	Damaging	0.19	Stabilizing
241	−0.46	Decrease	−1.561	Damaging	−1.499	Damaging
242	−0.3	Decrease	−1.574	Damaging	−1.512	Damaging
243	−0.35	Decrease	−1.331	Damaging	−1.096	Damaging
244	0.72	Enhance	−0.648	Damaging	−0.031	Damaging
245	0.18	Enhance	−1.09	Damaging	−0.83	Damaging
246	0.49	Enhance	−0.546	Damaging	−0.449	Damaging
248	0.04	Enhance	−0.272	Damaging	−0.104	Damaging
249	−2.05	Decrease	−0.901	Damaging	−0.916	Damaging
251	−1.56	Decrease	−0.543	Damaging	−0.551	Damaging
252	2.06	Enhance	−0.959	Damaging	−0.022	Damaging
253	−1.01	Decrease	−0.282	Damaging	−0.044	Damaging
254	−2.23	Decrease	−2.109	Highly damaging	−2.322	Damaging

(Cont'd...)

Table 2. *(Continued)*

Serial number	Computational server					
	SDM		mCSM		DUET	
	ΔΔG	Prediction of protein stability	ΔΔG	Prediction of protein stability	ΔΔG	Prediction of protein stability
255	−2.23	Decrease	−1.524	Damaging	−1.886	Damaging
256	−2.51	Decrease	−1.068	Damaging	−1.314	Damaging
257	−1.48	Decrease	−1.602	Damaging	−1.8	Damaging
258	−1.2	Decrease	−1.282	Damaging	−1.375	Damaging
259	0.62	Enhance	−2.554	Highly damaging	−2.103	Damaging
260	−1.37	Decrease	−2.77	Highly damaging	−2.94	Damaging
261	−2.75	Decrease	−0.921	Damaging	−1.194	Damaging
262	−0.6	Decrease	−1.188	Damaging	−1.162	Damaging
263	−1.8	Decrease	−2.268	Highly damaging	−2.523	Damaging
264	−0.25	Decrease	−1.212	Damaging	−1.028	Damaging
265	0.08	Enhance	−0.499	Damaging	−0.179	Damaging
266	−1.1	Decrease	−1.912	Damaging	−1.991	Damaging
267	−0.77	Decrease	−1.415	Damaging	−1.386	Damaging
269	0.39	Enhance	−0.398	Damaging	−0.124	Damaging
270	1.73	Enhance	−1.155	Damaging	−0.344	Damaging
271	−0.37	Decrease	−0.609	Damaging	−0.29	Damaging
272	−0.98	Decrease	−1.443	Damaging	−1.302	Damaging
273	−2.78	Decrease	−1.231	Damaging	−1.766	Damaging
274	−1.59	Decrease	−1.302	Damaging	−1.54	Damaging
275	−1.29	Decrease	0.235	Stabilizing	0.407	Stabilizing
276	−0.5	Decrease	−0.018	Damaging	0.31	Stabilizing
277	−0.85	Decrease	−0.131	Damaging	−0.098	Damaging
278	−0.3	Decrease	−0.162	Damaging	−0.04	Damaging
279	−0.46	Decrease	0.152	Stabilizing	0.096	Stabilizing
280	−0.31	Decrease	−0.642	Damaging	−0.45	Damaging
281	0.22	Enhance	−0.481	Damaging	−0.154	Damaging
283	−0.7	Decrease	−0.927	Damaging	−0.935	Damaging
284	−0.52	Decrease	0.043	Stabilizing	0.025	Stabilizing
285	−0.13	Decrease	−1.119	Damaging	−0.996	Damaging
286	−0.8	Decrease	−0.131	Damaging	−0.21	Damaging
287	−1.24	Decrease	0.335	Stabilizing	0.197	Stabilizing
288	−0.45	Decrease	−0.863	Damaging	−0.798	Damaging
289	−0.5	Decrease	−0.369	Damaging	−0.14	Damaging
290	−1.19	Decrease	−0.442	Damaging	−0.65	Damaging
291	0.86	Enhance	−1.18	Damaging	−0.745	Damaging
292	0.52	Enhance	−1.572	Damaging	−1.227	Damaging
293	0.58	Enhance	−0.397	Damaging	−0.006	Damaging
294	−0.5	Decrease	−1.064	Damaging	−1.231	Damaging
295	−0.44	Decrease	−1.581	Damaging	−1.556	Damaging
296	−0.71	Decrease	−1.476	Damaging	−1.407	Damaging
297	0.59	Enhance	−1.611	Damaging	−1.089	Damaging
298	−1.7	Decrease	−2.091	Highly damaging	−2.354	Damaging
299	−0.51	Decrease	−1.611	Damaging	−1.737	Damaging

Abbreviation: ΔΔG: Difference in free energy between the mutant and wild−type proteins.

Table 3. Predicted cancer-associated CXCR1 mutations using the FATHMM server

Serial number	Mutation	Prediction
44	R135C	Cancer
45	R135L	Cancer
46	R135H	Cancer
95	N57D	Cancer
208	P302S	Cancer

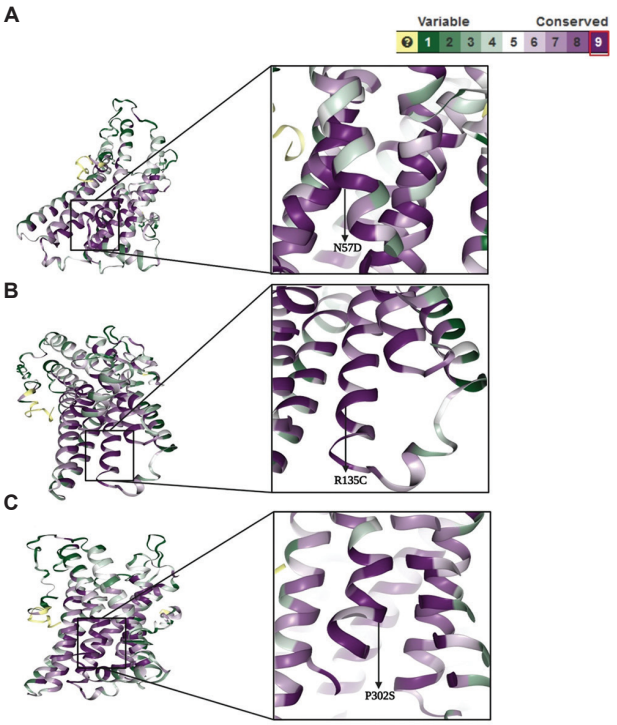


Figure 1. Residue conservation analysis of the N57D, R135C, and P302S residues of CXCR1 using the ConSurf server. (A) respresent that residues mutations N57D, (B) represent R135C, and (C) represent that P302S lyes in most consered regin of CXCR1 protein structure.

used to measure the model's quality.[65] The data revealed that 76.7% of the residues in the model were in the favored region of the native CXCR1 structure (Figure 2).

3.7. Molecular dynamic simulation of CXCR1

To understand the conformational changes caused by the N57D, R135C, and P302S mutations in the CXCR1 protein, a 100 ns MDS was performed. Various structural parameters, such as secondary structure elements (SSEs), were used to monitor the protein's behavior during the simulation.

The RMSD value can provide insight into the stability of protein structures. In this study, the RMSD was calculated for the backbone residues of the native and mutant CXCR1 proteins by comparing them with their original structures. As displayed in Figure 3A and C, the RMSD values for the mutant proteins (N57D, R135C, and P302S) were found to be highly unstable compared to those of the native protein. While the native protein remained stable during simulation, the mutant proteins took a longer time to stabilize. The RMSD values for the mutant proteins continuously increased from 25 to 45 ns, whereas the RMSD values for the native CXCR1 remained stable. These findings indicate that these mutations adversely affected protein stability and function. The RMSD for the mutant CXCR1 was approximately 8 Å (Figure 3C), while that for the native CXCR1 was approximately 4.4 Å (Figure 3A).

Next, we calculated the RMSF of the Cα atom to investigate the effect of mutated CXCR1 proteins on residue dynamics, i.e., protein stability and function. The RMSF values of the mutant structures were reportedly greater than those of the native structures, particularly for residues located between positions 150 and 200 (7.7 RMSF Å fluctuation) and between positions 300 and 350 (8 and 11 RMSF Å fluctuation) (Figure 4A and B).

3.8. Protein secondary structure elements

The SSE algorithm was used to investigate the structural flexibility of CXCR1 proteins.[60] Figure 5 displays the data on SSEs over time, allowing for a comparison of the structural changes between the native and mutant CXCR1 proteins. Both the native and mutant forms of the protein exhibited coils, α-helices, turns, bends, and β-sheets during the simulation. In contrast, the mutant protein displayed a significant rise in residues forming α-helices (Figure 5B), while the native protein exhibited a decrease in both loops and β-strands forming residues (Figure 5A).

3.9. Effects of mutant CXCR1 on protein secondary/tertiary structure elements

For homology modeling of normal and mutant CXCR1, the I-TASSER modeled structure was evaluated using UCSF Chimera calculations.[66] We performed homology modeling of the normal and mutant CXCR1 structures to assess the spatial arrangement of the conserved amino acids asparagine (N57), arginine (R135), and proline (P302), while the mutant amino acids included aspartic acid (57D), cysteine (135C), and serine (302S). This investigation was prompted by the observation of the highest sequence similarity and conserved sequence of CXCR1. We selected the structures of asparagine (N57), arginine (R135), and proline (P302), while the aspartic acid (57D), cysteine (135C), and serine (302S) mutants were used to generate a 3D model of CXCR1 using the I-TASSER online tool based on high C-scores. Notably, the C-score of the CXCR1

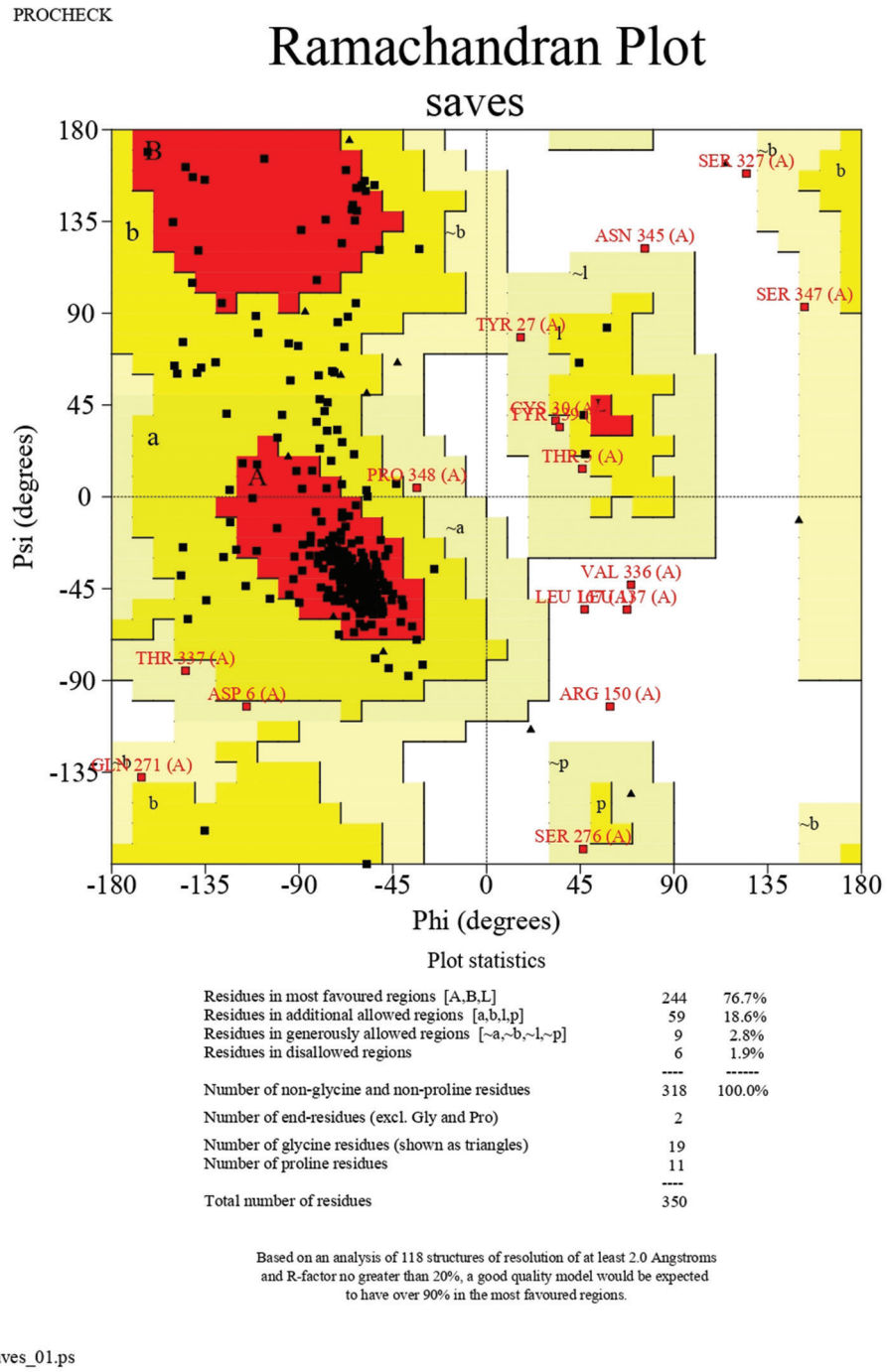


Figure 2. Ramachandran plot analysis to assess the quality of both native and mutant CXCR1 protein structures with a focus on the distribution of residues in the plot. The plot is displayed in a colored format to enable easier visualization.

normal line was -1.20, the template modeling score (TMS) was 0.56 ± 0.15, and the RMSD was 6.4 ± 3.9 Å, while the C-score of the CXCR1 mutant was -1.10, the TM-score was 0.54 ± 0.14, and the RMSD was 6.2 ± 3.7 Å.

The mutation of asparagine (N) to aspartic acid (D) in a protein induces changes in both secondary and tertiary structures. This difference is attributed to the distinct side-chain properties of the amino acids, facilitating local interactions and potentially altering the hydrogen bonding networks. The influence of mutations on electrostatic interactions and hydrophobic forces can further contribute to modifications in the overall folding and stability of

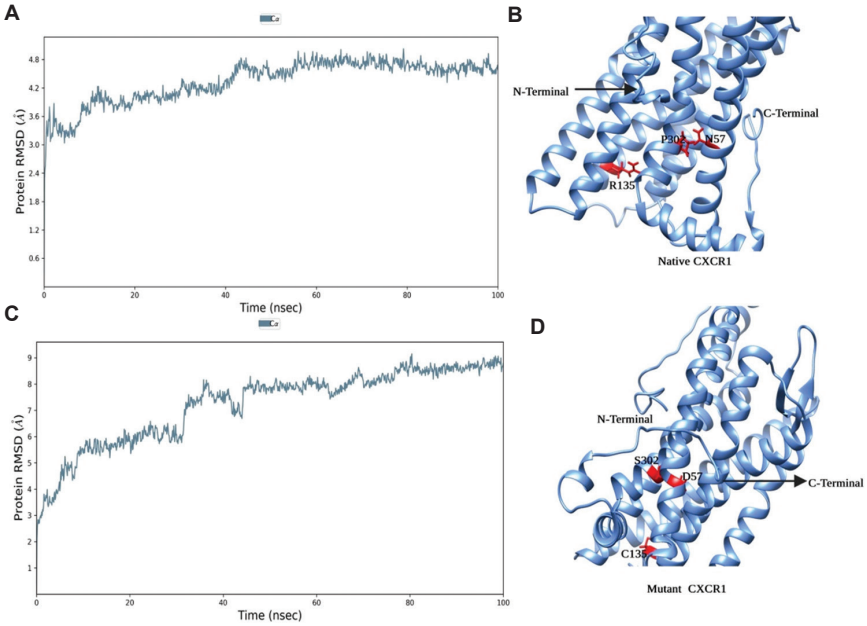


Figure 3. Molecular dynamic simulations of the native and mutant CXCR1 proteins over 100 ns and the backbone root-mean-square deviation (RMSD) of the two structures. (A) shows native protein remained stable during simulation with RMSD value of 4.4 Å. (B) represent normal 3D structure of CXCR1 with no effect on structure stability. (C) The RMSD values for mutant proteins N57D, R135C, and P302S, at 8 Å, indicate significant instability. (D) structure of CXCR1, post-point mutation, shows notable alterations, affecting protein stability and function.

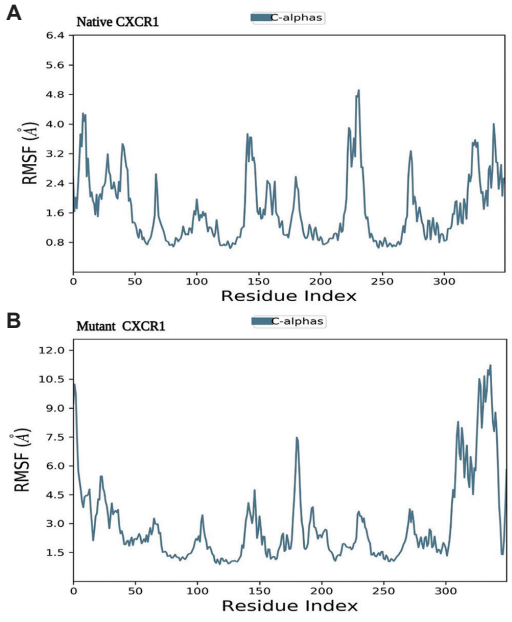


Figure 4. Analysis of the native CXCR1 protein structure following a molecular dynamic simulation. In terms of the root-mean-square fluctuation (RMSF) of the backbone alpha carbon (Cα) atoms over the simulation period. The y-axis of the plot represents the RMSF values, and the x-axis of the plot corresponds to each atom in the protein structure. (A) Represents lower RMSF values (4 Å fluctuation) notably for residues between positions 150 and 200, with values at positions 300 and 350 measuring 3.8 Å. (B) Shows higher RMSF values for mutant structures compared to native structures, with residues between positions 150 and 200 fluctuating at 7.7 Å and between positions 300 and 350 fluctuating at 8 and 11 Å, respectively.

proteins.[67] The changes in amino acid distances in the structure of the CXCR1 normal N57 and G56 amino acids was 5.9 Å, that of N57 and S58 was 10.4 Å, that of the D57 and G56 amino acids was 6.8 Å, and that of D57 with S58 was 9.7 Å (Figure 6A). The asparagine (N) at position 57 was likely involved in hydrogen bonding due to its polar nature. Substituting asparagine with aspartic acid (D) would introduce a negative charge. This change could disrupt hydrogen bonding interactions in the region, potentially affecting the local structure.

A point mutation of arginine (R) with cysteine (C) in a protein has notable effects on the secondary and tertiary structures. The differing side chain properties, including charge and length, disrupt local interactions, affecting the stability of secondary structures such as α-helices and β-sheets. In addition, this substitution can influence the overall 3D folding of the protein, altering its electrostatic interactions and potentially impacting its functional conformation.[68] In our study, the length of the normal CXCR1 R135 with D134 was 6.5 Å, the length of the R135 with the amino acid Y136 was 11.8 Å, the length of the C135 with D134 was 7.6 Å, and the length of the C135 with Y136 was 11 Å (Figure 6B). Arginine (R) at position 135 is a positively charged amino acid that may be involved in electrostatic interactions. Substituting arginine with cysteine (C) eliminates the positive charge and disrupts the protein's electrostatic interactions. In addition, cysteine

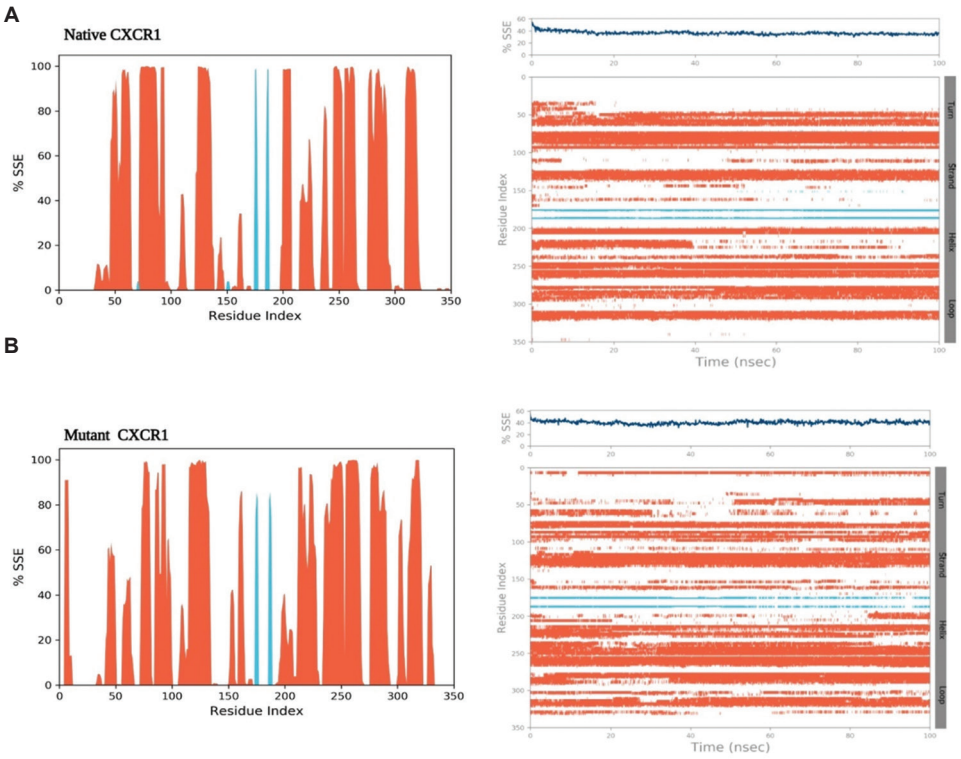


Figure 5. Time-dependent changes in the secondary structural element classification for both the native and mutant protein structures a 100-ns period. (A) Demonstrated a decrease in the residues forming both loops and β-strands. (B) Indicates a significant increase in residues forming α-helices.

can form disulfide bonds that can potentially alter the overall protein structure.

Substitution of proline (P) with serine (S) in a protein induces notable effects on both secondary and tertiary structures. When the cyclic, rigid side chain of proline is replaced with the flexible, hydroxyl-containing side chain of serine, the substitution disrupts the local conformations and regular secondary structures such as α-helices. At the tertiary level, the unique structural constraints imposed by proline are altered, influencing the overall 3D folding pattern of the protein.[69] In this study, the amino acid distances of the normal CXCR1 P302 amino acid with amino acids N301 and I303 were 6.7Å and 6.9Å, respectively (Figure 6C). In contrast, the amino acid distances of mutant CXCR1 S302 with N301 and I303 were 7.2Å and 8.9Å, respectively (Figure 6C). Nonetheless, structural variations were observed in terms of distance measurements and C-scores (Figure 6). These findings provided critical insights into the structural disparities and corresponding functional implications of CXCR1 among proteins and critical mutations.

4. Discussion

CXCR1 interacts with CXCL8 through its N-terminal β-strand.[17] The tertiary structures of the CXCL8 dimers were simulated in the present study. The CXCL8-CXCR1/2 signaling axis is implicated in the pathophysiology of various disorders, including chronic obstructive pulmonary disease (COPD), asthma, cystic fibrosis, and cancer. The interaction of CXCL8, which is released by some cancer cells, with CXCR1/2 in the tumor microenvironment is crucial in carcinogenesis and cancer metastasis.[6] Recent advancements in computational biology enabled the visualization of the disease status and genotype–phenotype association.[70] The integration of various bioinformatics approaches can identify potential missense mutations in genes that may have functional implications. This comprehensive methodology enables the exploration and detection of genetic variations that could impact the function and behavior of specific genes, thereby contributing to our understanding of their role in biological processes and disease development.[71] This study employed several bioinformatics methods to identify mutations in the CXCR1 gene that may be harmful and contribute to carcinogenesis. Through various analyses, we aimed to understand how these mutations could impact protein stability and function.

In the present study, by computational tools, 53 of the 299 mutations extracted from the public database were predicted to be deleterious (Table 1). Five mutations were

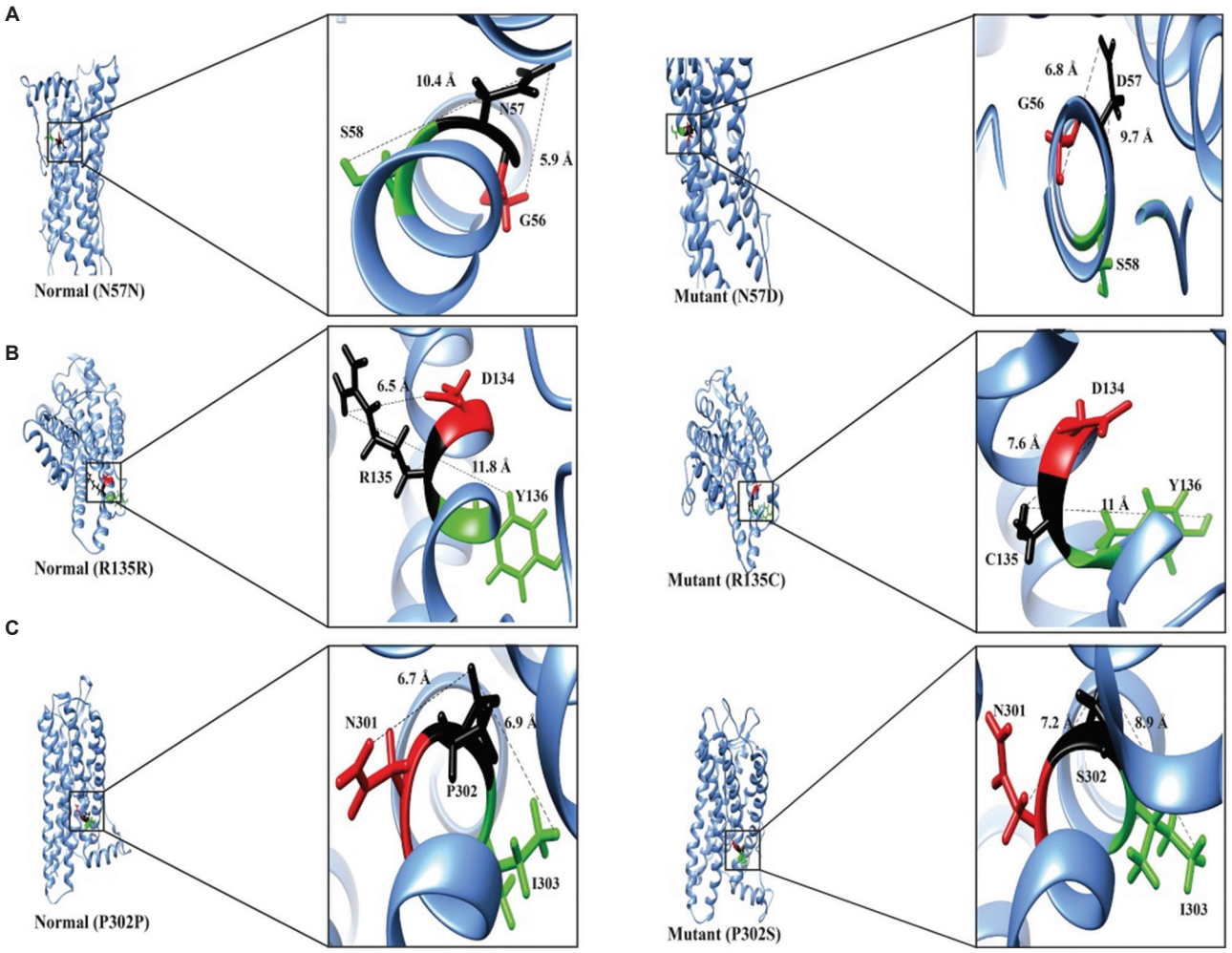


Figure 6. The structural impact of mutations on CXCR1, focusing on the conserved amino acids (N57, R135, and P302). (A) The asparagine (N) to aspartic acid (D) mutation at position 57 induced changes in amino acid distances, with N57–G56 at 5.9 Å and N57–S58 at 10.4 Å in the normal protein and D57–G56 at 6.8 Å and D57–S58 at 9.7 Å in the mutant protein. (B) The R-to-C mutation at position 135 exhibited alterations in bond distances, with R135–D134 at 6.5 Å and R135–Y136 at 11.8 Å in the normal protein and C135–D134 at 7.6 Å and C135–Y136 at 11 Å in the mutant protein. (C) The proline (P) to serine (S) mutation at position 302 exhibited variations in amino acid distances, with P302–N301 at 6.7 Å and P302–I303 at 6.9 Å in the normal protein and S302–N301 at 7.2 Å and S302–I303 at 8.9 Å in the mutant protein.

identified by FATHMM analysis as carcinogenic mutations (Table 3). We selected N57D, R135C, and P302S among the five mutations and conducted a conservation analysis that revealed the high conservation of the N57, R135, and P302 positions, with a conservation score of 9 (Figure 1A-C). A previous study revealed that the double mutants R199H/D265H and R203H/D265H, as well as the triple mutant R199H/R203H/D265H in CXCR1, failed to trigger an IL-8-dependent calcium response.[72] Interestingly, this mutation appears in the DRY motif and mostly resides in the TM region of CXCR1 for interaction with its ligands; it is also found at the IC end of TM3 in CXCR1, and it is also a highly conserved motif. The arginine residue (R) is conserved in 96% of receptors in this class.[73] The highly conserved DRY motif in CXCR1, particularly the conserved arginine residue (R), the TMs, TM1, TM3, and TM7, present promising opportunities for in-depth research to fully comprehend the influence of this motif on the structure, stability, and functionality of the protein.[74] Further investigations could shed light on how this motif contributes to the overall function of CXCR1.

Identifying the specific locus of the mutated amino acid can provide insight into how the mutation may alter the protein's overall structure and function. Numerous studies have examined how the location of mutations within a protein structure can affect its function. The relationships between mutation location and effects on protein structure, stability, and function have been investigated in

these studies to gain insights into disease development and progression.[23,75] Using I-TASSER, we modeled the native and mutant CXCR1 protein structures (Figure 3B and D) for MDS analysis to explore the structural consequences of the mutation on the protein structure. This approach allowed us to investigate the effect of the mutation on the overall structure of the protein. The RMSD data obtained from the simulations indicated that the mutant CXCR1 protein displayed a distinct and noticeable pattern of deviation throughout the entire simulation duration compared to the behavior observed for the native protein (Figure 3A and C). This finding suggested that the mutation significantly destabilized the CXCR1 protein, leading to structural alterations that are different from those observed in the native protein. The RMSF data provided additional evidence to corroborate the hypothesis that the mutation disrupts the stability of the protein structure (Figure 4A and B). The data revealed that the level of variation at the residue level was significantly greater in the mutant protein than in the wild-type protein, indicating that the mutation significantly altered the protein conformation and increased its flexibility. The SSE analysis indicated that the mutant protein exhibited a distinct alteration in the protein conformation, transitioning from an α-helix to a coil form, unlike the native protein (Figure 5A and B). This finding suggested that the mutation-induced changes in the protein's secondary structure, leading to a shift in its overall conformation. The observed conformational changes in our analysis offer compelling evidence that the substitution of amino acids in the mutant protein resulted in substantial alterations to its overall structure. These alterations resulted in mutant proteins that are less stable, more flexible, and less tightly packed than the native protein. Taken together, our results strongly indicated that the mutation had a significant and profound influence on both the structure and stability of the protein.

Previous studies have demonstrated the complementary nature of *in silico* approaches and wet laboratory experiments in understanding biological phenomena. The integration of computational methods with experimental techniques has proven to be a powerful tool for predicting and validating hypotheses in a range of biological systems.[70,76] The combination of computational mutation predictions with MDS analysis has been instrumental in identifying disease-causing mutations.[77] This approach has enabled the identification of the most deleterious mutations from a large pool of mutations, providing valuable insights into the molecular basis of various diseases.[78] Computational methods play a vital role in establishing the groundwork for genetic research aimed at comprehending the molecular foundations of diseases.[79] These methods facilitate the detection of mutations that contribute to diseases and assist in the exploration of potential therapeutic strategies. Moreover, such computational methods can assist in the clinical assessment of genetic variants,[70,76] enabling more informed and effective treatment decisions.

5. Conclusion

In silico investigations of the TM domains of CXCR1 (TM1, TM3, and TM7) revealed N57D, R135C, and P302S point mutations as potential carcinogenic variants. In addition, MDS analysis indicated that these mutations lead to changes in the structural stability of the protein, including increased flexibility and reduced compactness. The structural instability of the mutant protein could lead to an inability to interact with the CXCL8 ligand and other associated proteins, which may have implications for cancer development. The molecular understanding attained through this study could serve as a foundation for *in vitro* and *in vivo* experiments investigating the effect of N57D, R135C, and P302S mutations on the interaction of CXCR1 with its ligand and its association with disease development.

Acknowledgments

None.

Funding

This work was supported by the National Natural Science Foundation of China (32270438, 32170498, 31970388), National Key Research and Development Program of China (2021YFF0702000, 2018YFD0900602), 1.3.5 Project for Disciplines of Excellence by the West China Hospital, Sichuan University (ZYJC21050), Science and Technology Department of Sichuan Province (2022YFH0116), Priority Academic Program Development of Jiangsu Higher Education Institutions (PAPD), and the National Clinical Research Center for Geriatrics, West China Hospital, Sichuan University (Z2023JC003).

Conflict of interest

The authors declare no conflict of interest.

Author contributions

Conceptualization: Shah Kamal, Gohar Mushtaq, Muhammad Nasir Iqbal

Formal analysis: Shah Kamal, Amanullah Amanullah, Qingqing Wang, Najeeb Ullah, Muhammad Nasir Iqbal

Writing – original draft: Shah Kamal, Gohar Mushtaq, Mohammad Amjad Kamal

Writing – review & editing: Gohar Mushtaq, Mohammad Amjad Kamal, Najeeb Ullah

Ethics approval and consent to participate

Not applicable.

Consent for publication

Not applicable.

Availability of data

All datasets generated for this study are available on request from the corresponding authors.

References

1. Yang D, Zhou Q, Labroska V, *et al*. G protein-coupled receptors: Structure-and function-based drug discovery. *Signal Transduct Target Ther.* 2021;6(1):7.

   doi: 10.1038/s41392-020-00435-w

2. Katritch V, Cherezov V, Stevens RC. Diversity and modularity of G protein-coupled receptor structures. *Trends Pharmacol Sci.* 2012;33(1):17-27.

   doi: 10.1016/j.tips.2011.09.003

3. Berman HM, Westbrook J, Feng Z, *et al*. The protein data bank. *Nucleic Acids Res.* 2000;28(1):235-242.

   doi: 10.1093/nar/28.1.235

4. Rajagopalan L, Rajarathnam K. Ligand selectivity and affinity of chemokine receptor CXCR1. Role of N-terminal domain. *J Biol Chem.* 2004;279(29):30000-30008.

   doi: 10.1074/jbc.M313883200

5. Holmes WE, Lee J, Kuang WJ, Rice GC, Wood WI. Structure and functional expression of a human interleukin-8 receptor. Science. 1991;253(5025):1278-1280. *J Immun.* 2009;183(5):2895-2897.

   doi: 10.1126/science.1840701

6. Ha H, Debnath B, Neamati N. Role of the CXCL8-CXCR1/2 axis in cancer and inflammatory diseases. *Theranostics.* 2017;7(6):1543-1588.

   doi: 10.7150/thno.15625

7. Park SH, Das BB, Casagrande F, *et al*. Structure of the chemokine receptor CXCR1 in phospholipid bilayers. *Nature.* 2012;491(7426):779-783.

   doi: 10.1038/nature11580

8. Sojka AC, Brennan KM, Maizels ET, Young CD. The science behind g protein-coupled receptors (GPCRs) and their accurate visual representation in scientific research. *J Biocommun.* 2017;41(1):e6.

   doi: 10.5210/jbc.v41i1.7309

9. Hofmann KP, Scheerer P, Hildebrand PW, *et al*. A G protein-coupled receptor at work: The rhodopsin model. *Trends Biochem Sci.* 2009;34(11):540-552.

   doi: 10.1016/j.tibs.2009.07.005

10. Park JH, Scheerer P, Hofmann KP, Choe HW, Ernst OP. Crystal structure of the ligand-free G-protein-coupled receptor opsin. *Nature.* 2008;454(7201):183-187.

    doi: 10.1038/nature07063

11. Vauquelin G, Van Liefde I. G protein-coupled receptors: A count of 1001 conformations. *Fundam Clin Pharmacol.* 2005;19(1):45-56.

    doi: 10.1111/j.1472-8206.2005.00319.x

12. Rosenbaum DM, Rasmussen SGF, Kobilka BK. The structure and function of G-protein-coupled receptors. *Nature.* 2009;459(7245):356-363.

    doi: 10.1038/nature08144

13. Rosenbaum DM, Cherezov V, Hanson MA, *et al*. GPCR engineering yields high-resolution structural insights into beta2-adrenergic receptor function. *Science.* 2007;318(5854):1266-1273.

    doi: 10.1126/science.1150609

14. Landau EM, Rosenbusch JP. Lipidic cubic phases: A novel concept for the crystallization of membrane proteins. *Proc Natl Acad Sci U S A.* 1996;93(25):14532-14535.

    doi: 10.1073/pnas.93.25.14532

15. Oldham WM, Hamm HE. Heterotrimeric G protein activation by G-protein-coupled receptors. *Nat Rev Mol Cell Biol.* 2008;9(1):60-71.

    doi: 10.1038/nrm2299

16. Leong SR, Kabakoff RC, Hébert CA. Complete mutagenesis of the extracellular domain of interleukin-8 (IL-8) type A receptor identifies charged residues mediating IL-8 binding and signal transduction. *J Biol Chem.* 1994;269(30):19343-19348.

17. Skelton NJ, Quan C, Reilly D, Lowman H. Structure of a CXC chemokine-receptor fragment in complex with interleukin-8. *Structure.* 1999;7(2):157-168.

    doi: 10.1016/S0969-2126(99)80022-7

18. Hébert CA, Vitangcol RV, Baker JB. Scanning mutagenesis of interleukin-8 identifies a cluster of residues required for receptor binding. *J Biol Chem.* 1991;266(28):18989-18994.

19. Nicholls DJ, Tomkinson NP, Wiley KE, *et al*. Identification of a putative intracellular allosteric antagonist binding-site in the CXC chemokine receptors 1 and 2. *Mol Pharmacol.* 2008;74(5):1193-1202.

    doi: 10.1124/mol.107.044610

20. Han X, Feng Y, Chen X, Gerard C, Boisvert WA. Characterization of G protein coupling mediated by the conserved D134(3.49) of DRY motif, M241(6.34), and F251(6.44) residues on human CXCR1. *FEBS Open Bio.* 2015;5:182-190.

    doi: 10.1016/j.fob.2015.03.001

21. Huynh N, Mallik B, Zhang L, Martins-Green M, Morikis D. Computational studies of CXCR1, the receptor of IL-8/CXCL8, using molecular dynamics and electrostatics. *Biopolymers.* 2008;89(1):52-61.

doi: 10.1002/bip.20851

22. Pandurangan AP, Blundell TL. Prediction of impacts of mutations on protein structure and interactions: SDM, a statistical approach, and mCSM, using machine learning. *Protein Sci.* 2020;29(1):247-257.

doi: 10.1002/pro.3774

23. Capriotti E, Altman RB, Bromberg Y. Collective judgment predicts disease-associated single nucleotide variants. *BMC Genomics.* 2013;14(Suppl 3):S2.

doi: 10.1186/1471-2164-14-S3-S2

24. López-Ferrando V, Gazzo A, de la Cruz X, Orozco M, Gelpí JL. PMut: A web-based tool for the annotation of pathological variants on proteins, 2017 update. *Nucleic Acids Res.* 2017;45(W1):W222-W228.

doi: 10.1093/nar/gkx313

25. Choi Y, Chan AP. PROVEAN web server: A tool to predict the functional effect of amino acid substitutions and indels. *Bioinformatics.* 2015;31(16):2745-2747.

doi: 10.1093/bioinformatics/btv195

26. Rogers MF, Shihab HA, Mort M, Cooper DN, Gaunt TR, Campbell C. FATHMM-XF: Accurate prediction of pathogenic point mutations via extended features. *Bioinformatics.* 2018;34(3):511-513.

doi: 10.1093/bioinformatics/btx536

27. Pires DE, Ascher DB, Blundell TL. mCSM: Predicting the effects of mutations in proteins using graph-based signatures. *Bioinformatics.* 2014;30(3):335-342.

doi: 10.1093/bioinformatics/btt691

28. Worth CL, Preissner R, Blundell TL. SDM--a server for predicting effects of mutations on protein stability and malfunction. *Nucleic Acids Res.* 2011;39:W215-222.

doi: 10.1093/nar/gkr363

29. Pires DE, Ascher DB, Blundell TL. DUET: A server for predicting effects of mutations on protein stability using an integrated computational approach. *Nucleic Acids Res.* 2014;42:W314-W319.

doi: 10.1093/nar/gku411

30. Martin FJ, Amode MR, Aneja A, *et al.* Ensembl 2023. *Nucleic Acids Res.* 2023;51(D1):D933-D941.

doi: 10.1093/nar/gkac958

31. Sherry ST, Ward MH, Kholodov M, *et al.* dbSNP: The NCBI database of genetic variation. *Nucleic Acids Res.* 2001;29(1):308-311.

doi: 10.1093/nar/29.1.308

32. UniProt Consortium. UniProt: A hub for protein information. *Nucleic Acids Res.* 2015;43:D204-D212.

doi: 10.1093/nar/gku989

33. Goodsell DS, Zardecki C, Di Costanzo L, *et al.* RCSB protein data bank: Enabling biomedical research and drug discovery. *Protein Sci.* 2020;29(1):52-65.

doi: 10.1002/pro.3730

34. Hecht M, Bromberg Y, Rost B. Better prediction of functional effects for sequence variants. *BMC Genomics.* 2015;16(Suppl 8):S1.

doi: 10.1186/1471-2164-16-S8-S1

35. Mi H, Lazareva-Ulitsky B, Loo R, *et al.* The PANTHER database of protein families, subfamilies, functions and pathways. *Nucleic Acids Res.* 2005;33:D284-D288.

doi: 10.1093/nar/gki078

36. Ng PC, Henikoff S. SIFT: Predicting amino acid changes that affect protein function. *Nucleic Acids Res.* 2003;31(13):3812-3814.

doi: 10.1093/nar/gkg509

37. Bendl J, Stourac J, Salanda O, *et al.* PredictSNP: Robust and accurate consensus classifier for prediction of disease-related mutations. *PLoS Comput Biol.* 2014;10(1):e1003440.

doi: 10.1371/journal.pcbi.1003440

38. Pejaver V, Mooney SD, Radivojac P. Missense variant pathogenicity predictors generalize well across a range of function-specific prediction challenges. *Hum Mutat.* 2017;38(9):1092-1108.

doi: 10.1002/humu.23258

39. Ghosh M, Sodhi SS, Sharma N, *et al.* An integrated *in silico* approach for functional and structural impact of non-synonymous SNPs in the MYH1 gene in Jeju Native Pigs. *BMC Genet.* 2016;17:35.

doi: 10.1186/s12863-016-0341-1

40. Vila JA. Proteins' evolution upon point mutations. *ACS Omega.* 2022;7(16):14371-14376.

doi: 10.1021/acsomega.2c01407

41. Pandurangan AP, Ochoa-Montaño B, Ascher DB, Blundell TL. SDM: A server for predicting effects of mutations on protein stability. *Nucleic Acids Res.* 2017;45(W1):W229-W235.

doi: 10.1093/nar/gkx439

42. Choudhury A, Mohammad T, Anjum F, *et al.* Comparative analysis of web-based programs for single amino acid substitutions in proteins. *PLoS One.* 2022;17(5):e0267084.

doi: 10.1371/journal.pone.0267084

43. AlAjmi MF, Khan S, Choudhury A, *et al.* Impact of deleterious mutations on structure, function and stability of serum/glucocorticoid regulated kinase 1: A gene to diseases correlation. *Front Mol Biosci.* 2021;8:780284.

doi: 10.3389/fmolb.2021.780284

44. Rodrigues CHM, Myung Y, Pires DEV, Ascher DB. mCSM-PPI2: Predicting the effects of mutations on protein-protein interactions. *Nucleic Acids Res.* 2019;47(W1):W338-W344.

doi: 10.1093/nar/gkz383

45. Mutlu G, Acı Çİ. SVM-SMO-SGD: A hybrid-parallel support vector machine algorithm using sequential minimal optimization with stochastic gradient descent. *Parallel Comput.* 2022;113:102955.

doi: 10.1016/j.parco.2022.102955

46. Shihab HA, Gough J, Cooper DN, Day INM, Gaunt TR. Predicting the functional consequences of cancer-associated amino acid substitutions. *Bioinformatics.* 2013;29(12):1504-1510.

doi: 10.1093/bioinformatics/btt182

47. Zhang Y. I-TASSER server for protein 3D structure prediction. *BMC Bioinformats.* 2008;9:40.

doi: 10.1186/1471-2105-9-40

48. Ishimoto N, Park JH, Kawakami K, *et al*. Structural basis of CXC chemokine receptor 1 ligand binding and activation. *Nat Commun*. 2023;14(1):4107.

doi: 10.1038/s41467-023-39799-2

49. Lovell SC, Davis IW, Arendall WB 3rd, *et al*. Structure validation by Calpha geometry: Phi,psi and Cbeta deviation. *Proteins*. 2003;50(3):437-450.

doi: 10.1002/prot.10286

50. Kc DB. Recent advances in sequence-based protein structure prediction. *Brief Bioinform.* 2017;18(6):1021-1032.

doi: 10.1093/bib/bbw070

51. Hollingsworth SA, Dror RO. Molecular Dynamics Simulation for All. *Neuron.* 2018;99(6):1129-1143.

doi: 10.1016/j.neuron.2018.08.011

52. Muhammed MT, Aki-Yalcin E. Homology modeling in drug discovery: Overview, current applications, and future perspectives. *Chem Biol Drug Des*. 2019;93(1):12-20.

doi: 10.1111/cbdd.13388

53. Brooks BR, Brooks CL 3rd, Mackerell AD Jr, *et al*. CHARMM: The biomolecular simulation program. *J Comput Chem.* 2009;30(10):1545-1614.

doi: 10.1002/jcc.21287

54. Rasheed MA, Iqbal MN, Saddick S, *et al*. Identification of lead compounds against Scm (fms10) in *Enterococcus faecium* using computer aided drug designing. *Life (Basel).* 2021;11(2):77.

doi: 10.3390/life11020077

55. Hildebrand PW, Rose AS, Tiemann JKS. Bringing molecular dynamics simulation data into view. *Trends Biochem Sci.* 2019;44(11):902-913.

doi: 10.1016/j.tibs.2019.06.004

56. Ferreira LG, Dos Santos RN, Oliva G, Andricopulo AD. Molecular docking and structure-based drug design strategies. *Molecules.* 2015;20(7):13384-13421.

doi: 10.3390/molecules200713384

57. Shivakumar D, Williams J, Wu Y, Damm W, Shelley J, Sherman W. Prediction of absolute solvation free energies using molecular dynamics free energy perturbation and the OPLS force field. *J Chem Theory Comput.* 2010;6(5):1509-1519.

doi: 10.1021/ct900587b

58. Huang Y, Li Z, Hong Q, *et al*. A stepwise docking molecular dynamics approach for simulating antibody recognition with substantial conformational changes. *Comput Struct Biotechnol J.* 2022;20:710-720.

doi: 10.1016/j.csbj.2022.01.012

59. Hung LH, Guerquin M, Samudrala R. GPU-Q-J, a fast method for calculating root mean square deviation (RMSD) after optimal superposition. *BMC Res Notes.* 2011;4:97.

doi: 10.1186/1756-0500-4-97

60. Carter P, Andersen CAF, Rost B. DSSPcont: Continuous secondary structure assignments for proteins. *Nucleic Acids Res.* 2003;31(13):3293-3295.

doi: 10.1093/nar/gkg626

61. Ashkenazy H, Abadi S, Martz E, *et al*. ConSurf 2016: An improved methodology to estimate and visualize evolutionary conservation in macromolecules. *Nucleic Acids Res.* 2016;44(W1):W344-W350.

doi: 10.1093/nar/gkw408

62. Wang Y, Park JH, Lupala CS, *et al*. Computer aided protein engineering to enhance the thermo-stability of CXCR1-T4 lysozyme complex. *Sci Rep.* 2019;9(1):5317.

doi: 10.1038/s41598-019-41838-2

63. Yang J, Zhang Y. Protein structure and function prediction using I-TASSER. *Curr Protoc Bioinformatics.* 2015;52:5.8.1-5.8.15.

doi: 10.1002/0471250953.bi0508s52

64. Roy A, Kucukural A, Zhang Y. I-TASSER: A unified platform for automated protein structure and function prediction. *Nat Protoc.* 2010;5(4):725-738.

doi: 10.1038/nprot.2010.5

65. Sobolev OV, Afonine PV, Moriarty NW, *et al*. A global Ramachandran score identifies protein structures with unlikely stereochemistry. *Structure.* 2020;28(11):1249-1258.e2.

doi: 10.1016/j.str.2020.08.005

66. Guzzi AF, Oliveira FSL, Amaro MMS, Tavares-Filho PF, Gabriel JE. *In silico* prediction of the functional and structural consequences of the non-synonymous single nucleotide polymorphism A122V in bovine CXC chemokine receptor

type 1. *Braz J Biol.* 2020;80(1):39-46.

doi: 10.1590/1519-6984.188655

67. Kato K, Nakayoshi T, Kurimoto E, Oda A. Mechanisms of deamidation of asparagine residues and effects of main-chain conformation on activation energy. *Int J Mol Sci.* 2020;21(19):7035.

doi: 10.3390/ijms21197035

68. Chakkalakal SA, Heilig J, Baumann U, Paulsson M, Zaucke F. Impact of arginine to cysteine mutations in collagen II on protein secretion and cell survival. *Int J Mol Sci.* 2018;19(2):541.

doi: 10.3390/ijms19020541

69. Ganguly HK, Basu G. Conformational landscape of substituted prolines. *Biophys Rev.* 2020;12(1):25-39.

doi: 10.1007/s12551-020-00621-8

70. Zaki OK, Krishnamoorthy N, El Abd HS, *et al.* Two patients with Canavan disease and structural modeling of a novel mutation. *Metab Brain Dis.* 2017;32(1):171-177.

doi: 10.1007/s11011-016-9896-9

71. Agrahari AK, Kumar A, Siva R, Zayed H, Doss CGP. Substitution impact of highly conserved arginine residue at position 75 in GJB1 gene in association with X-linked Charcot-Marie-tooth disease: A computational study. *J Theor Biol.* 2018;437:305-317.

doi: 10.1016/j.jtbi.2017.10.028

72. Suetomi K, Rojo D, Navarro J. Identification of a signal transduction switch in the chemokine receptor CXCR1. *J Biol Chem.* 2002;277(35):31563-31566.

doi: 10.1074/jbc.M204713200

73. Mirzadegan T, Benkö G, Filipek S, Palczewski K. Sequence analyses of G-protein-coupled receptors: Similarities to rhodopsin. *Biochemistry.* 2003;42(10):2759-2767.

doi: 10.1021/bi027224+

74. Rovati GE, Capra V, Neubig RR. The highly conserved DRY motif of class A G protein-coupled receptors: Beyond the ground state. *Mol Pharmacol.* 2007;71(4):959-964.

doi: 10.1124/mol.106.029470

75. Arshad M, Bhatti A, John P. Identification and *in silico* analysis of functional SNPs of human TAGAP protein: A comprehensive study. *PLoS One.* 2018;13(1):e0188143.

doi: 10.1371/journal.pone.0188143

76. Mosaeilhy A, Mohamed MM, Doss CGP, *et al.* Genotype-phenotype correlation in 18 Egyptian patients with glutaric acidemia type I. *Metab Brain Dis.* 2017;32(5):1417-1426.

doi: 10.1007/s11011-017-0006-4

77. Zhao F, Zheng L, Goncearenco A, Panchenko AR, Li M. Computational approaches to prioritize cancer driver missense mutations. *Int J Mol Sci.* 2018;19(7):2113.

doi: 10.3390/ijms19072113

78. Chun S, Fay JC. Identification of deleterious mutations within three human genomes. *Genome Res.* 2009;19(9):1553-1561.

doi: 10.1101/gr.092619.109.

79. Li J, Wei Z, Hakonarson H. Application of computational methods in genetic study of inflammatory bowel disease. *World J Gastroenterol.* 2016;22(3):949-960.

doi: 10.3748/wjg.v22.i3.949